

ATTITUDE CONTROL AND ORBIT DETERMINATION OF A CREWED SPACECRAFT WITH LUNAR LANDER IN NEAR RECTILINEAR HALO ORBIT

Clark P. Newman,^{*} Ryan Sieling[†], Diane C. Davis[‡], and Ryan J. Whitley^{**}

NASA's Gateway program plans to place a crew-tended spacecraft in cislunar Near Rectilinear Halo Orbit (NRHO). The craft will support arrivals of crews in Orion and the undocking and return of a crewed lunar lander. The impact to attitude control of a Gateway with the addition of a lunar lander is investigated. Perturbations from Orion and a lander's docking and undocking from the Gateway are considered. Deep Space Network (DSN) tracking is supplemented with optical measurements to lunar north pole craters to analyze the possible benefit in solution accuracy and/or DSN scheduling relief.

INTRODUCTION

The Gateway is envisioned as a part of an evolutionary expansion of human presence beyond Earth orbit, an outpost in cis-lunar space. From its orbit near the Moon, the Gateway will support crewed visits, missions to the lunar surface, or missions into heliocentric space. It will be constructed on-orbit with elements launched individually or as comanifested payloads with an Orion spacecraft. Proposed configurations include a human lunar lander comprised of three components, docked robotically to the Gateway in successive missions. After the arrival of a crewed Orion at the Gateway, the crew will board the lander and depart for the lunar surface.

The Gateway is planned to orbit in an Earth-Moon Near Rectilinear Halo Orbit (NRHO). An NRHO is a halo orbit that exhibits nearly stable behavior and lies nearly normal to the Earth-Moon orbital plane. The specific NRHO targeted for this mission is the 9:2 Lunar-Synodic Resonant (LSR) southern L2 NRHO. The orbit's apolune is ~70,000 km below the Moon, with the perilune radius of about 3200 km oriented above the lunar north pole. The plane of the NRHO remains nearly normal to the Earth-Moon vector in the rotating Earth-Moon frame.^{1,2}

While in orbit, the Gateway will be subject to the dynamical environment of cislunar space. Solar radiation pressure will push and torque the Gateway, and the gravity gradient from a highly eccentric orbit will torque the spacecraft. The Gateway is planned to maintain its NRHO with orbit maintenance maneuvers (OMMs) executed at apolune.³⁻⁶ Docking contact forces and visiting vehicle thruster plumes will impart torques and translational forces on the Gateway. During crewed Orion visits, periodic vents will also push and torque the Gateway. Attitude will be maintained and angular momentum disturbances will be absorbed by the Control Moment Gyros (CMGs), which require desaturation maneuvers. Executed by the reaction

^{*} Senior Systems Engineer, a.i. solutions, Inc., 2224 Bay Area Blvd, Houston TX 77058.

[†] Principal Systems Engineer, a.i. solutions, Inc., 2224 Bay Area Blvd, Houston TX 77058.

[‡] Principal Systems Engineer, a.i. solutions, Inc., 2224 Bay Area Blvd, Houston TX 77058.

^{**} Deputy Systems Integration Manager, Exploration Mission Planning Office, NASA Johnson Space Center, 2101 NASA Parkway, Houston, Texas 77058.

control system (RCS), the desaturation burns will expend hydrazine and perturb the spacecraft. These errors and perturbations are considered in dynamic simulations of the Gateway on-orbit.

In this paper, the progressive construction of the Gateway is simulated to examine the propellant use over time as the spacecraft’s mass properties and response to perturbations changes. A propellant budget is built from this five-year timeline of construction and extrapolated from its completion through a fifteen year mission. A hypothetical lunar lander mission is simulated, with Orion bringing crew to a completed Gateway, who board and depart the Gateway in the lander. After one revolution of the Gateway in NRHO, the ascent element of the lander returns to the Gateway, and the crew move back into the Orion and depart after apolune. The total propellant cost of mitigating perturbations from these dockings and undockings, as well as a look into a waived lander mission, are extracted from simulations.

A crewed mission to the Gateway, including a lunar lander scenario, is depicted in Figure 1. The arriving Orion spacecraft follows the outbound trajectory on the right in green, performing a powered flyby of the Moon before rendezvous with Gateway in the blue NRHO after perilune. The crew descends to Low Lunar Orbit (LLO) along the orange path prior to the subsequent perilune passage, and then to the lunar surface. After a stay of approximately six days, the ascent element returns to the Gateway, following the orange trajectory to rendezvous after perilune. The crew departs the Gateway in Orion after the subsequent apolune passage, following the green return trajectory back to Earth.

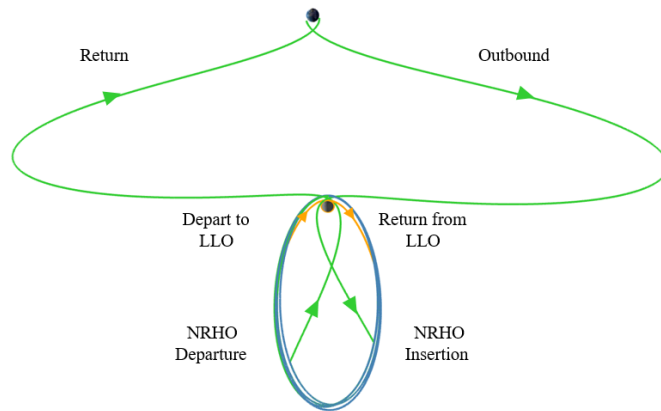


Figure 1. Trajectories to/from NRHO and to/from LLO as seen in the rotating Earth-Moon frame.

Throughout the lifetime of the mission, the Gateway will be tracked and will communicate to Earth via the Deep Space Network (DSN). The DSN provides range and range rate measurements, which are fed into a Square Root Information Filter (SRIF) to estimate the Gateway’s state. The DSN is chronically over-scheduled, and discrepancies in tracking can affect mission performance. Any effort to supplement DSN tracking with autonomous methods may result in reduced reliance on the DSN and increased mission robustness. Visual measurements of craters could supplement DSN tracking to improve the state resolution or to reduce scheduling with the DSN without sacrificing orbit determination (OD) performance. The Gateway passes over the north pole at perilune, and a camera fixed to the $-Z$ side of the Gateway could capture and measure northern lunar craters as Gateway passes over. Such measurements are fed into the SRIF to reduce the state uncertainty. A maneuver estimation error is defined, and the maneuver estimation error is analyzed for different tracking schedules.

MODELING

Two main simulations are discussed in this paper: an attitude dynamics simulation and an orbit determination simulation. The force modeling in each case is identical, except for the specific applications of the respective simulations. That is, there is no flat plate model computing solar torques in the OD simulation, nor is a SRIF active in the attitude dynamics simulation.

The Gateway is propagated numerically in a gravity field that includes the Earth, Moon, and Sun. The Moon is modeled with spherical harmonic gravity field of degree and order 8, while the Sun and Earth are

modeled as point masses. Solar radiation pressure is included, and in the attitude dynamics simulation SRP torques are summed over a flat plate model to integrate angular momentum changes.

The Gateway maintains its NRHO with OMMs executed at apolune. OMMs are calculated by targeting the x component of the rotating velocity, v_x , along a reference trajectory in the Earth Moon rotating frame. A receding horizon of 6.5 revolutions is selected to target v_x at perilune passages.⁴ Nominally an OMM is executed every apolune, but in practice targeted OMMs that fall below a threshold are waived to avoid the necessary slews and time spent in off-nominal attitudes. A previous investigation shows that skipping maneuvers with a magnitude below a threshold of 3 cm/s does not raise the total cost of stationkeeping.⁷

The modeling of Gateway is imperfect, so errors and random perturbations are included and Monte Carlo analysis conducted to capture the averages and dispersions of orbit maintenance and attitude maintenance propellant use. In the attitude dynamics simulation, the Gateway state is subject to navigation error once per revolution at the OMM. The OMM itself is subject to pointing and magnitude error. In the OD simulation, the OMM with pointing and magnitude error is executed on a truth spacecraft while the estimated spacecraft executes a perfect OMM. Perturbations affect both simulations and include body-fixed perturbations like docking plume and contact reactions, as well as body-fixed venting events. Random perturbations occur with RCS thruster firings for momentum desaturations and RCS thruster-controlled slews. A summary of modeling errors and perturbations appears in Table 1.

Angular Momentum Modeling

In the attitude dynamics simulation, the Gateway’s mass properties and physical dimensions are configurable through the addition and placement of elements and spacecraft. Adding an element places its mass properties in the body frame, and a set of flat plates bounds the element’s form. Solar pressure imparts torques and translational forces on the Gateway’s flat plates, while the combined mass properties are torqued by lunar gravity gradient. The change in momentum from these torques are integrated while the attitude is held as an input in the simulation. Explicitly, the attitude dynamics simulation is not a full six degree of freedom simulation and attitude is considered an input.

The flat plate model places plates bounding each element into position in the Gateway body frame. Each plate is defined by its position in space, its normal unit vector, its area, and three coefficients of reflectivity. The coefficients of reflectivity follow

$$R_{\text{spec}} + R_{\text{diff}} + R_{\text{abs}} = 1 \tag{1}$$

where the coefficients in Equation 1 represent specular reflection, diffuse reflection, and absorption, respectively. Plates in the simulation are specified as either body plates or solar panel plates to model their disparate reflective properties. Errors applied to the values of these coefficients capture the uncertainty inherent in modeling reflective properties of complex spacecraft surfaces.

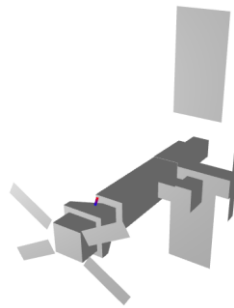


Figure 2. Depiction of flat plate model of configuration 12. The wastewater vent vector is visible on Orion, originating in blue and pointing toward red.

Torques applied to the Gateway are compensated with control torques from the CMG set that exists in the first Gateway element, the Power and Propulsion Element (PPE). The momentum carried by the CMG set is tracked through integration of the input torques. The CMG set is assumed to consist of four wheels arranged in an equilateral isosceles pyramid. The momentum capacity envelope of the system is assumed to

be spherical and have a maximum capacity of 1.633 times the momentum capacity of a single wheel in any direction.⁹ It is assumed that each single wheel has 250Nms of momentum capacity in a single axis, so the CMG set has 408Nms of capacity in each body axis.

The Gateway reaction control system (RCS) thrusters perform desaturation maneuvers, crewed slews, and crewed OMMs. The RCS is assumed to consist of 16 thrusters on the corners of the radial PPE faces, canted at an angle to optimize pitch and yaw maneuvers. Four additional thrusters are assumed to exist on the aft panel for OMM execution. Each RCS thruster is modeled as a hydrazine-fueled 20N thruster with an Isp of 200s. CMG desaturation maneuvers are modeled as impulsive and are automatically triggered by the CMG momentum reaching a threshold. RCS slews are modeled as impulsive burns with finite attitude transitions. As the Gateway attitude changes over time, the CMG set absorbs SRP torques.

An Orion requirement drives the use of RCS thrusters for crewed slews and OMMs. Orion is required to maintain a tail-to-sun attitude with a maximum excursion of three hours. For an OMM sequence, the Gateway must slew to the burn attitude, execute the burn, and slew back to tail-to-sun attitude within the three hour limit. The slews are budgeted 75 minutes each and the OMM is budgeted 30 minutes to meet this requirement. The maximum slew time drives the required slew rate of the Gateway during crewed operations, necessitating RCS thrusters. Similarly, increased perturbations from a crewed Gateway lead to larger OMM magnitudes that require more than the allotted 30 minutes for SEP execution, forcing the task to the high-thrust RCS thrusters.

For this simulation, a variable slew rate was implemented to reduce hydrazine use. Originally, the slew rate was set to execute a 180 degree slew in 75 minutes to satisfy Orion’s tail-to-Sun requirement. However, hydrazine cost per slew is a function of slew rate: you must torque up to achieve the slew rate, then torque back down to come to rest at the desired attitude. Moving forward, slews executed with RCS thrusters will have their slew rates scaled per slew to execute all slews with a fixed time of 75 minutes, rather than a fixed rate. As the Sun circles the rotating Earth-Moon system, slews to stationkeeping attitude over time average out to 90 degrees, so on average the slew rate is reduced by half.

These activities and others cause perturbations to the Gateway velocity and to its angular momentum. Errors are placed on parameters and states of the simulation and processed in a Monte Carlo execution to capture the range of behavior and propellant use for attitude operations. Errors and perturbations are specified in Tables 1 and 2. For each error or perturbation source in Table 1, the phase of the mission in which it is active is listed, along with the 3-sigma magnitude that is seeded, the frequency the error is applied, and in what direction if specified. Table 2 shows the same parameters for perturbations that have constant values. Desaturation maneuvers are triggered automatically, so the desaturation rate varies between Gateway configurations, the presence of Orion, and location in the orbit. A desaturation maneuver is commanded regardless of CMG status at apolune before OMM execution.

Table 1. Error models for crewed and uncrewed spacecraft configurations.

<i>Error/Perturbation</i>	<i>Phases</i>	<i>3-sigma value</i>	<i>Frequency</i>	<i>Direction</i>
Insertion error	Initial	20 km, 20 cm/s	At insertion	Random
Navigation error	All	10 km, 10 cm/s	At each OMM	Random
SRP panel error	All	15% R_{spec} , 15% R_{diff}	At insertion	Random
Attitude error	All	1 deg	After every slew	Random
Desaturation perturbation	Uncrewed	3 cm/s	Variable	Random
OMM execution error: SEP	Uncrewed	1.42 mm/s + 1.5%	At each SEP OMM	Random
Desaturation perturbation	Crewed	3 cm/s	Variable	Random
OMM execution error: RCS	Crewed	1%	At each RCS OMM	Random

Table 2. Constant perturbation models for crewed and uncrewed spacecraft configurations

<i>Error/Perturbation</i>	<i>Phases</i>	<i>Constant value</i>	<i>Frequency</i>	<i>Direction</i>
Docking perturbation	Dock + undock	0.1 m/s	At dock + undock	{-1, 0, 0} body-fixed
RCS slew perturbation	Crewed	1.883e-2 kgm/s	Pre and post-OMM	Random
CO ₂ puff perturbation	1 st Crewed Configuration	22.54 kgm/s	10 min	{-0.5, -0.866, 0.0} body-fixed
Wastewater dump perturbation	Crewed	51.20 kgm/s	3 hours	{-0.5, 0.0, -0.866} body-fixed

As Tables 1 and 2 show, the crewed phase introduces more errors and perturbations. Docking, RCS slewing, and venting perturbations all exert torque, which is absorbed by the CMGs, increasing the desaturation rate. Additionally, the added mass of Orion increases the torques exerted on the Gateway from the lunar gravity gradient. CO₂ vents from Orion are only applied during the first crewed mission. The next crewed mission brings the first crew habitat, which is assumed to carry air recirculation with zero net force vents.

GATEWAY CONSTRUCTION SIMULATION

The Gateway will be constructed on station in the NRHO with each element delivered either independently or as a comanifested payload with an Orion mission. While the Gateway grows in mass and volume as each element is added, it is currently assumed that all the attitude control systems will be located in the PPE only. To inform the initial PPE propellant requirement, an analysis into a lifetime fuel budget is performed.

The Gateway is planned to be constructed through several missions over the course of five years, after which it is considered complete and will continue its mission for another ten years. It is assumed in these ten years there will be one crewed mission to the Gateway per year. A crewed mission to the completed Gateway may also include a lunar lander excursion, discussed in the next section. Table 3 summarizes one pathway in which the Gateway can be constructed. In this construction path, the first element to arrive on station is the PPE, inserted on arrival into the target NRHO. The next element to be installed is the *Espirit / USUM Element (EUE)*, arriving as a comanifested payload with Orion in configuration 2. *Logistics Vehicle 1 (LV1)* arrives independently prior to the next Orion mission, delivering food and supplies to the Gateway in configuration 4. Orion then arrives, comanifested with the first habitat element, in configuration 5. A second habitat arrives with the next Orion mission (configuration 7), before LV1 is deployed on a safe disposal path (configuration 8). A second *Logistics Vehicle* arrives and supports the Orion mission with the *Multipurpose Module (MPM)* as comanifested payload (configurations 10 and 11). At this point the Gateway is considered complete and will nominally support ten years of missions.

Table 3. Simulated construction path of the Gateway.

<i>Config</i>	<i>Mass (MT)</i>	<i>Duration (revolutions)</i>
1	8	56
2	39.4	1
3	16	45
4	30	8
5	62.4	4
6	39	51
7	71.4	4
8	48	1
9	39	40
10	53	8
11	85.4	0
12	85.4	4
13	62	2
14 (G1)	52.7	50

Moments of Inertia and Slewing

As the Gateway adds elements, a major impact on attitude control is the moments of inertia of each stack configuration. As seen in Figure 3, the moments of inertia of the Gateway tend to rise as each element is added, with large increases due to Orion dockings. The main driver for slow speeds for either CMGs or RCS is the moments of inertia of the Gateway. As the Gateway grows, the maximum slewing speeds will decrease for both CMG and RCS control. For larger configurations, especially crewed configurations, RCS control is necessary.

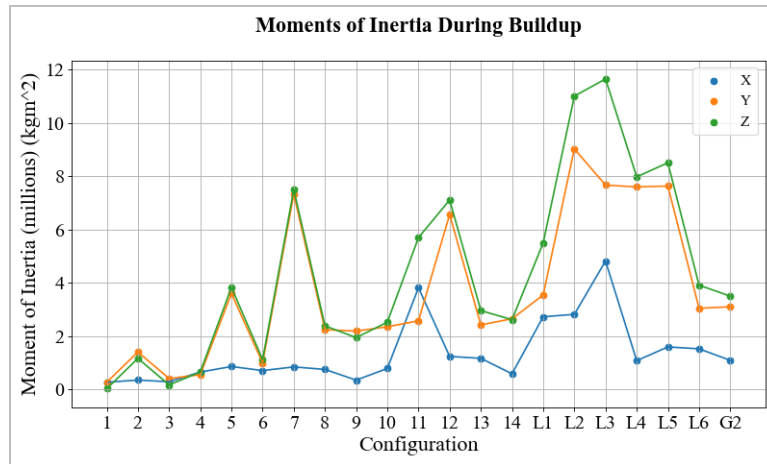


Figure 3. Moments of inertia for each configuration.

CMG System

The limiting factors for slewing with the CMGs are the angular momentum capacity and available torque of the system in any axis. The angular momentum determines the maximum slew speed of the Gateway, and the torque determines how quickly the Gateway can reach that maximum speed. For large slews with smaller wheels on a large configuration, the maximum speed is the limiting factor. Using the momentum value of the nominal CMGs, and the moments of inertia of the Gateway, a theoretical maximum rotation speed can be calculated for each configuration, as seen in Figure 4.

The main reason for slewing is to adjust attitude for an orbit maintenance burn; slews vary from 0 to 180 degrees. For a slew of 180 degrees about the axis associated with the maximum moment of inertia for each configuration, a worst-case approximation for rotation times is computed and appears in Figure 4. The rotation time for a given angle is directly proportional to both the wheel speed and the moment of inertia. Only uncrewed configurations are included, as the slew speeds associated with the CMGs are too slow to slew the Gateway and satisfy the tail-to-sun Orion requirement.

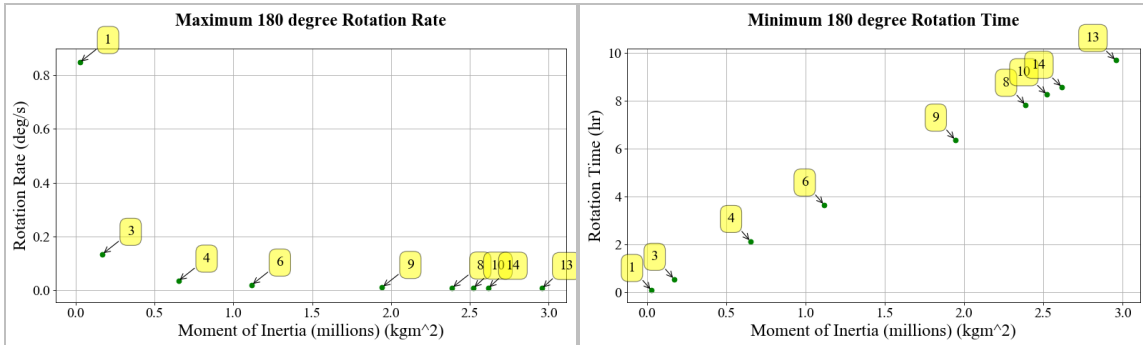


Figure 4. Rotation rate (left) and time (right) for a 180 degree slew in each uncrewed configuration's largest axis with CMGs.

The rotation rates and times in Figure 4 are based on theoretical slews with no external torques. In reality, a number of torques, namely SRP torques, accumulate during the slew. The resultant momentum is stored in the CMGs after the slew. If the slew is too slow, the accumulation of SRP torque saturates the wheels, and a desaturation burn must occur. Above some inertia thresholds, smaller wheels are unable to perform large slews without saturating, no matter how slow the slew is.

RCS Thrusters

For RCS thrusters, the rotation rate is limited by the torque output by the thruster configuration. The quickest possible slew is executed by a maximum torque in one direction until the halfway point, followed by a torque in the opposite direction until the desired rotation is met. This slew execution results in the smallest rotation time and largest average rotation speed, but it also requires the most fuel. Assuming four 20 N thrusters orthogonal to the surface at the ends of the PPE, a maximum torque of approximately 180 Nm is computed. Applying this to a 180-degree rotation yields the maximum rotation rate for a 180 degree slew as well as the corresponding minimum rotation time. Values appear in Figure 5 for the Gateway configurations summarized in Table 3.

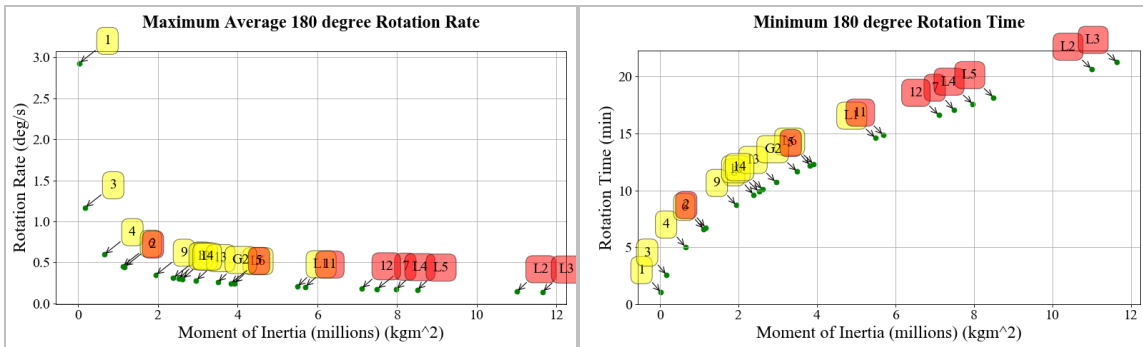


Figure 5. Rotation rate (left) and time (right) for 180 degree slews in each uncrewed (yellow) and crewed (red) configuration's largest axis with RCS thrusters.

Using specific impulse and the ideal rocket equation, fuel estimates are computed for the minimum slew time, as seen in Figure 6 on the left. Since this is the quickest possible slew, the fuel use is at a maximum. Rotating the Gateway this fast will not likely be necessary, and slower slews save fuel. Due to the Orion tail-to-sun requirement, the Gateway must slew at least 180 degrees in 75 minutes, or 0.04 deg/s.

Using this as the average rotation rate, a minimum fuel usage is approximated for each slew, seen in Figure 6 on the right.

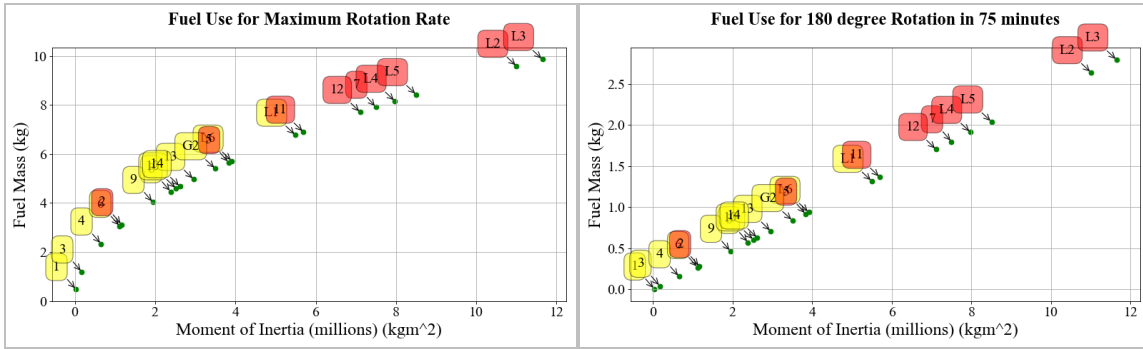


Figure 6. Maximum (left) and nominal (right) fuel use for 180 degree slews for each uncrewed (yellow) and crewed (red) configuration's largest axis.

Fuel Budget of a Gateway Construction Path

To capture a hydrazine propellant budget for the duration of the Gateway’s construction, each configuration is simulated in a Monte Carlo analysis and the average and maximum hydrazine propellant use are calculated and averaged over the number of revolutions. With propellant use rates for each configuration, a schedule of construction determines how long each configuration persists in the construction, and a total budget is calculated. The results of the Monte Carlo analysis appear in Table 4. The average and maximum values of hydrazine propellant per revolution appear in the table, along with the number of revolutions allocated to each configuration, and the resulting total hydrazine used for the duration of each configuration. The crewed configurations (configurations 2, 5, 7, and 12) are highlighted in bold text. The hydrazine use per revolution for the uncrewed configurations, which only use hydrazine for desaturation burns, is much lower than for the crewed configurations. The per-revolution hydrazine use for configuration 2 is by far the highest, due to the CO₂ puffs executed every 10 minutes by Orion. This short 10-day mission with a relatively lightweight stack requires nearly as much propellant as the later 30-day missions with much heavier stacks. This large propellant use demonstrates the value of moving the responsibility for air refreshment from the Orion spacecraft to the Gateway habitat.

Momentum desaturation behavior influences propellant usage. Momentum desaturation maneuvers are triggered automatically as the CMGs reach their momentum capacity, and it is important to understand if desaturations are being triggered excessively, or if their placement is adversely impacting stationkeeping costs. The average and maximum number of desaturation maneuvers (desats) per revolution are calculated from Monte Carlo results and also appear in Table 4. Again, the maximum desaturation rate is associated with the first crewed mission to the Gateway, and the rate is driven by the CO₂ venting from Orion. This large desat rate implies that the stack attitude maintenance in configuration 2 should be executed by the RCS thrusters, not the CMGs. Removing the CO₂ venting reduces the desaturation rate by a significant factor. Crewed configurations 5, 7, and 12 still experience a high rate of desats, with the drivers identified as wastewater dumps from Orion and the gravity gradient torques over perilune.

It should be noted that there is a tighter distribution of desaturation rates as compared to hydrazine fuel use rates. Most crewed configurations have the mean and max number of desaturations per revolution to be nearly equal, while the hydrazine use rate changes more significantly. The simulation’s angular momentum integration is insensitive to random perturbations, which mostly act on the velocity of the Gateway. The venting schedule is pre-determined, and the gravity gradient torques are the same for each Monte Carlo iteration. It is the velocity perturbations which cause trajectory errors that must be mitigated with increased stationkeeping maneuver magnitudes. The stationkeeping costs differences between iterations drives the higher variance on hydrazine use per revolution.

Uncrewed stacks experience a much lower rate of desaturation events. Configurations 1 and 3 only require the single commanded desat prior to the OMM. As the stack grows, additional desats are triggered by

the gravity gradient torques, with an additional three to four desats occurring near perilune. The desaturation rate for uncrewed configurations levels off after configuration 6. Orion brings the second habitat with configuration 7, and this becomes the maximum length that Gateway achieves. From there, additional elements are mounted radially and actually reduce the differences between the principal moments of inertia, and it is the differences in these moments of inertia that drive gravity gradient torques.

Table 4. Desaturation maneuvers per revolution, hydrazine fuel used per revolution, and hydrazine fuel budget for the five-year construction phase of Gateway.

<i>Config</i>	<i>Avg Desats</i>	<i>Max Desats</i>	<i>Avg hydrazine per rev (kg)</i>	<i>Max hydrazine per rev (kg)</i>	<i>Revs</i>	<i>Total Avg (kg)</i>	<i>Total Max (kg)</i>
1	1.0	1.0	0.04	0.05	56	2.4	2.5
2	171.4	178.0	39.3	46.0	1	39.3	46.0
3	1.0	1.0	0.01	0.01	45	0.64	0.69
4	1.9	2.1	0.14	0.16	8	1.12	1.3
5	42.3	43.0	11.0	13.0	4	44.4	52.0
6	4.7	4.9	0.44	0.47	51	21.3	22.5
7	83.2	84.5	14.8	17.9	4	59.2	71.6
8	4.2	4.7	0.40	0.45	1	0.45	0.51
9	4.2	4.4	0.39	0.42	40	17.7	18.9
10	4.1	4.8	0.38	0.44	8	3.04	3.5
12	78.2	80.8	12.3	16.2	4	49.2	64.8
13	3.7	3.9	0.35	0.37	2	0.7	0.74
14 (G1)	4.0	4.2	0.38	0.41	50	20	23
<i>Five Year Total:</i>					274	259	308

The final three configurations listed in Table 4, configurations 12-14, represent an Orion mission arriving and completing the construction of Gateway. Configuration 11 is omitted in the fuel budget, it is a transitory configuration to document the Orion delivery of the airlock to the radial port before repositioning to the axial port of Configuration 12. The final configuration is given the second moniker “G1” to represent a completed uncrewed Gateway that remains in orbit long-term between Orion missions. When the Gateway is fully constructed, it is assumed to support Orion missions with four-revolution stays. The last three lines of Table 3 illustrate the configurations of a post-construction Orion mission. Starting from a completed and uncrewed Gateway, a crewed mission is first preceded by an uncrewed logistics element (LE) arrival (configuration 13). The Logistics element brings supplies and experiments to support the subsequent Orion arrival. Orion arrives and remains docked axially for four revolutions (configuration 12). After Orion departs and returns to Earth, the LE undocks and is disposed into heliocentric space (configuration 14). This cycle repeats for subsequent Orion missions to the Gateway. It is assumed missions will arrive at Gateway post-completion once per year. As such, a year of a constructed Gateway supporting a crewed Orion mission, using the fuel rates listed in Table 4, requires a hydrazine propellant budget between 69 and 89 kg. A 15-year budget assuming a 5-year construction period followed by 10 years of annual 30-day crewed missions appears in Table 5.

Table 5. 15-year Gateway hydrazine budget; no lander sequence.

<i>Description</i>	<i>Duration (years)</i>	<i>Mean hydrazine mass: total (kg)</i>	<i>Max hydrazine mass: total (kg)</i>
First 5 years of stack buildup	5	259	308
10 years of configs 12, 13, 14, repeated	10	699	885
<i>15-year total</i>	15	958	1193

Construction without Venting

The crewed configurations of the Gateway are notably more dynamic and expensive, and a significant contributor to this cost are the vents and waste water dumps from Orion. While it’s assumed that the first habitat element to arrive will have equipment to mitigate CO₂ venting from Orion, it is not yet decided whether a waste water management process will be available with the first or second habitat. The waste water dumps from Orion impart a torque on the Gateway which requires periodic desaturation maneuvers.

If the water dumps were designed to be torqueless or mitigated altogether, it could result in significant hydrazine savings that could drive the decision whether to include it.

The crewed configurations in the construction path were simulated again without waste water dumps on configurations 5, 7, and 12. Configuration 2 does not bring a habitat and is still assumed to vent CO₂ and dump waste water per Table 2. The resulting construction fuel budget is shown below in Table 6. Again the crewed configurations are in bold.

Table 6. Desaturation maneuvers per revolution, hydrazine fuel used per revolution, and hydrazine fuel budget for the five-year construction phase of Gateway assuming no venting after configuration 2.

<i>Config</i>	<i>Avg Desats</i>	<i>Max Desats</i>	<i>Avg hydrazine per rev (kg)</i>	<i>Max hydrazine per rev (kg)</i>	<i>Revs</i>	<i>Total Avg (kg)</i>	<i>Total Max (kg)</i>
1	1.0	1.0	0.04	0.05	56	2.4	2.5
2	171.4	178.0	39.3	46.0	1	39.3	46.0
3	1.0	1.0	0.01	0.01	45	0.64	0.69
4	1.9	2.1	0.14	0.16	8	1.12	1.3
5	13.0	13.5	5.9	7.8	4	23.5	31.4
6	4.7	4.9	0.44	0.47	51	21.3	22.5
7	13.3	13.5	7.5	9.4	4	29.9	37.8
8	4.2	4.7	0.40	0.45	1	0.45	0.51
9	4.2	4.4	0.39	0.42	40	17.7	18.9
10	4.1	4.8	0.38	0.44	8	3.04	3.5
12	10.9	11.0	8.2	11.4	4	32.9	45.6
13	3.7	3.9	0.35	0.37	2	0.7	0.74
14 (G1)	4.0	4.2	0.38	0.41	50	20	23
<i>Five Year Total:</i>					274	194	236

The total fuel budget mean and max reduced by 65 and 72 kg, respectively. Relatively, the hydrazine use rate is cut nearly in half by mitigating water dump torques. Perhaps the more salient finding is the significant reduction in desaturation maneuver counts over each revolution. The repeated firings and motion of the CMGs may be an unnecessary stress on critical hardware. Desaturation maneuvers may also disrupt operations or contaminate exterior surfaces. Finally, an issue preventing a timely desaturation maneuver could result in a loss of attitude control. Regardless, the crewed configurations still have a higher desaturation rate than the uncrewed configurations. This is due to the added mass of Orion being located on the axial docking port- extending the geometry of the Gateway and skewing the principal moments of inertia.

LANDER MISSION SIMULATION

When the Gateway is fully constructed, it may support an excursion to the lunar surface using a Human Lunar Lander (HLL). The lunar lander mission as currently envisioned employs a three-piece lander with a disposable descent element, a reusable ascent element, and a reusable space tug that tows the lander from NRHO to Low Lunar Orbit (LLO). A lander mission is preceded by the robotic delivery of the lander ascent and descent elements, the space tug, and a LE. The LE may bring fuel for the ascent and descent elements, and the order of arrival for the lander and tug elements may vary.

The mission begins from lander configuration L1, where Orion docks prior to apolune, bringing the Gateway to configuration L2. The Descent Element (DE) and Tug are moved to assemble the lander in configuration L3 before the lander departs to LLO prior to perilune, with the Gateway in configuration L4. After one additional revolution in the NRHO, the Ascent Element (AE) returns after perilune and docks to Hab1, setting the Gateway to configuration L5. Finally, after the subsequent apolune, Orion departs and the Gateway ends the lunar mission in configuration L6.

The lunar lander descent element and tug are assumed to arrive individually via commercial launches. Once the lander mission has concluded, the logistics element is disposed into heliocentric space. At a later time when the orbits re-align, the tug transfers to NRHO for rendezvous with the Gateway. This final event leaves the Gateway in a long-term configuration that includes a dry tug and a dry ascent element.

Fuel Budget for Construction Phase

By combining the initial assembly of the lander, the execution of the lander mission, and the return to a long-term inter-mission configuration, a propellant budget is compiled that captures lander missions through the lifetime of Gateway. Statistics from Monte Carlo simulations of the initial and subsequent lunar lander missions appear in Tables 6 and 7. The average and maximum desaturation rates for each configuration is included, along with the average and maximum hydrazine propellant use rates. Extrapolating these rates out for the ascribed mission durations, an average and maximum propellant budget is computed, considering the errors and perturbations as described in Table 1 and 2. Tables 6 and 7 contain the hydrazine propellant use totals for a year in which the human lunar lander is assembled and a lander mission is executed, and for a subsequent year in which two of the three dry lander elements remain on the Gateway until an Orion mission arrives with the ascent element and propellant for executing another lander mission.

Table 6. Desaturation maneuver per revolution and propellant budget statistics for one year including the initial lunar lander assembly and mission.

<i>Config</i>	<i>Avg desats</i>	<i>Max desats</i>	<i>Avg (kg)</i>	<i>Max (kg)</i>	<i>Revs</i>	<i>Total Avg (kg)</i>	<i>Total Max (kg)</i>
14	4.0	4.2	0.38	0.41	28	10.6	11.5
14 + DE	4.2	4.5	0.40	0.43	8	3.2	3.4
14 + DE + Tug	4.4	4.8	0.41	0.45	8	3.3	3.6
L1	4.3	4.7	0.45	0.50	8	3.6	4.0
Mission: L2-L5	varies	varies	12.9	16.9	3	51.2	60.8
<i>One-year totals:</i>					55	71.9	83.3

Table 7. Desaturation maneuvers per revolution and propellant budget statistics for one year including a subsequent lunar lander mission.

<i>Config</i>	<i>Avg desats</i>	<i>Max desats</i>	<i>Avg (kg)</i>	<i>Max (kg)</i>	<i>Revs</i>	<i>Total Avg (kg)</i>	<i>Total Max (kg)</i>
G2	4.5	4.7	0.42	0.45	45	18.9	20.3
G2 + LM	4.5	4.8	0.49	0.54	8	3.9	4.3
Mission: L3-L5	varies	varies	12.9	16.9	3	49.9	62.9
<i>One-year totals:</i>					54	72.7	87.5

Waived Landing Simulation Results

It is important to capture the impact to the attitude control system and hydrazine propellant budget if the lunar lander mission is waived after the crew has arrived in Orion. In this scenario, a technical or other problem scrubs the departure of the lander, so the massive configuration L2 remains assembled for multiple revolutions. For this analysis, a Monte Carlo simulation of the crewed mission with an aborted landing sequence is processed. The desaturation rate and propellant budget statistics from this analysis appear in Table 8.

Table 8. Desaturation rate statistics and hydrazine fuel budget statistics for a waived lunar landing mission.

<i>Config</i>	<i>Avg desats</i>	<i>Max desats</i>	<i>Avg (kg)</i>	<i>Max (kg)</i>	<i>Revs</i>	<i>Total Avg (kg)</i>	<i>Total Max (kg)</i>
14	4.0	4.2	0.38	0.41	37	10.6	11.5
14+DE	4.2	4.5	0.40	0.43	8	3.2	3.4
14+DE+Tug	4.4	4.8	0.41	0.45	8	3.28	3.6
L2	61.5	63.3	15.8	22.8	3	47.4	68.3
<i>One-year totals:</i>					56	64.5	86.8

The propellant use for a waived lunar landing is less than for a nominal mission. The desaturation rates for the L2 configuration are actually lower than that of configuration 12, but still much higher than uncrewed configurations. The reduction of docking and undocking perturbations associated with the lander

elements departing and returning reduce the stationkeeping costs during the crewed portions of the mission. The aborted lunar lander mission more closely resembles a three-revolution crewed configuration.

Total Propellant Budget

The lifetime of the Gateway is assumed to be 15 years. The Gateway lifecycle begins with a 5-year construction path that includes both crewed and uncrewed configurations, followed by 10 annual crewed missions after construction is complete. A number of the crewed missions end at the Gateway, with others carrying on to the lunar surface. The end-to-end lifetime hydrazine budget for the Gateway is scoped to evaluate the necessity for refueling and the appropriate values for initial fueling requirements. A spectrum of possible propellant budgets appear in Table 8. Every budget assumes the same 5-year construction path described in Table 4. Subsequently, the ten remaining crewed missions are split between lunar lander missions or Gateway missions. The number of lander missions defines each column of Table 9. Because the average lander sequence requires slightly more propellant than the average 30-day crewed Gateway mission, the average hydrazine costs increase slightly as the proportion of lander missions increases. However, the difference is not large; each lander scenario requires only about 2 kg of hydrazine more than a 30-day crewed stay on Gateway, and the maximum hydrazine use decreases slightly when an additional lander mission replaces a 30-day Gateway stay.

Table 9. End to end hydrazine fuel budgets for the Gateway assuming different numbers of lunar lander missions.

	Number of Lunar Surface Missions										
	0	1	2	3	4	5	6	7	8	9	10
Average (kg)	958	960	963	966	968	970	973	976	979	982	985
Max (kg)	1193	1188	1187	1186	1185	1184	1183	1182	1181	1180	1179

The hydrazine propellant budget does not change significantly depending on the mix of Gateway or Lunar surface missions. These budgets inform the decision to size the PPE’s initial loadout of hydrazine, or to include the opportunity for the PPE to receive hydrazine from a visiting vehicle. Finally, while beyond the scope of the current investigation, it is worth exploring possible hydrazine savings by incorporating the Orion’s thrusters with the PPE RCS system for an integrated attitude control system that leverages the full geometry of the Gateway.

Recall that if water dumps are mitigated for crewed configurations after a habitat shows up, then the construction pathway hydrazine costs could be expected to reduce by an average of 65 kg. That represents approximately 6.5% of the smallest total average hydrazine fuel budget.

ORBIT DETERMINATION CONSIDERATIONS

The Gateway is expected to be tracked entirely or in part by the Deep Space Network (DSN), a trio of ground tracking sites designed to provide coverage to deep space missions in most directions from Earth. The NRHO is always in view of the Earth and has a nearly repeating path as viewed from Earth, so tracking passes can be scheduled and linked to orbit position to provide predictable behavior. The DSN is chronically under scheduling stress, but navigation error has a direct correlation to stationkeeping fuel costs⁷, so a desirable tracking schedule that provides measurements to most effectively reduce stationkeeping propellant costs is desirable.

For this study, an OD simulation is developed and executed in a Monte Carlo process to investigate tracking schedules and resulting maneuver estimation errors and propellant costs. Maneuver estimation error is defined as the difference between the targeted stationkeeping maneuver for the true and estimated spacecraft. The DSN sites are simulated, and different tracking schedules are designed based on eight-hour passes. The Gateway itself is modeled as a point mass that experiences velocity perturbations per Table 1. Two Gateway spacecraft are simulated, one representing the true state of the Gateway and the second simulating the estimated Gateway state. The estimated Gateway’s state is processed with DSN range and range rate measurements through a Square Root Information Filter (SRIF).

The Gateway is assumed to be in an uncrewed configuration, and the truth and estimated Gateway states are processed through the simulation. Measurements are taken on the truth spacecraft, then processed to resolve the estimated spacecraft's state. The truth spacecraft is simulated with a higher fidelity lunar gravity model to approximate errors from gravity mismodeling. Angular momentum is not integrated in the OD simulation, so desaturation maneuvers and perturbations are prescribed into the simulation. Impulsive perturbations such as vents and desaturations are applied to the truth spacecraft only, while the covariance of the estimated spacecraft is increased with each perturbation to model the uncertainty in the state due to the event.

The first analysis assumes two eight-hour DSN tracking passes per revolution, and compares maneuver estimation error performance for different placement of the passes. The locations of the passes for three test cases appear in Figure 9. The first case centers each pass around apolune and perilune, the second case centers the passes in the inbound and outbound legs of the NRHO, and the third case places both passes consecutively before the maneuver estimation epoch. Each tracking schedule is simulated over nine uncrewed revolutions to include all solar orientations, and their maneuver estimation errors and stationkeeping costs are compared.

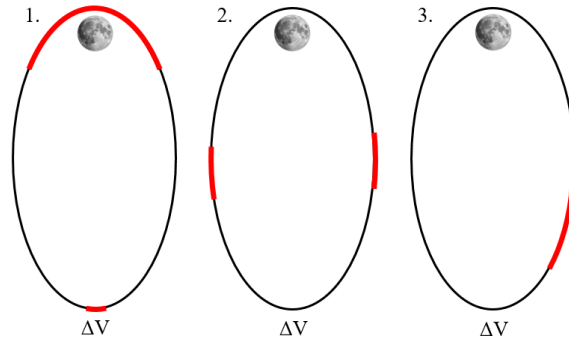


Figure 7. Locations of the tracking passes along the NRHO for each tracking case.

A time history of the Gateway's position and velocity uncertainty as computed by the SRIF for each tracking schedule appears in Figure 10 for a single case. Position is plotted in blue and measured in km, while velocity appears in red and is measured in cm/s. The bold lines represent times that the Gateway is being tracked by the DSN. Generally, uncertainty spikes in the neighborhood of perilune. It is also when the orbit shape is most sensitive to velocity perturbations. Recall from earlier that gravity gradient induced momentum desaturation maneuvers also occur near perilune, so velocity perturbations are expected in this neighborhood of high sensitivity and uncertainty.

The lowest overall uncertainty is achieved with the first tracking schedule, which includes the pass over perilune that inhibits the spike of uncertainty at the closest approach to the Moon. The largest uncertainty spikes occur in tracking schedule 3 during perilune passage, with velocity uncertainty exceeding 10 m/s and position uncertainty nearing 100 km. While the three tracking schedules yield significantly different uncertainties at perilune, the filter output does not vary significantly near apolune, where orbit maintenance maneuvers take place.

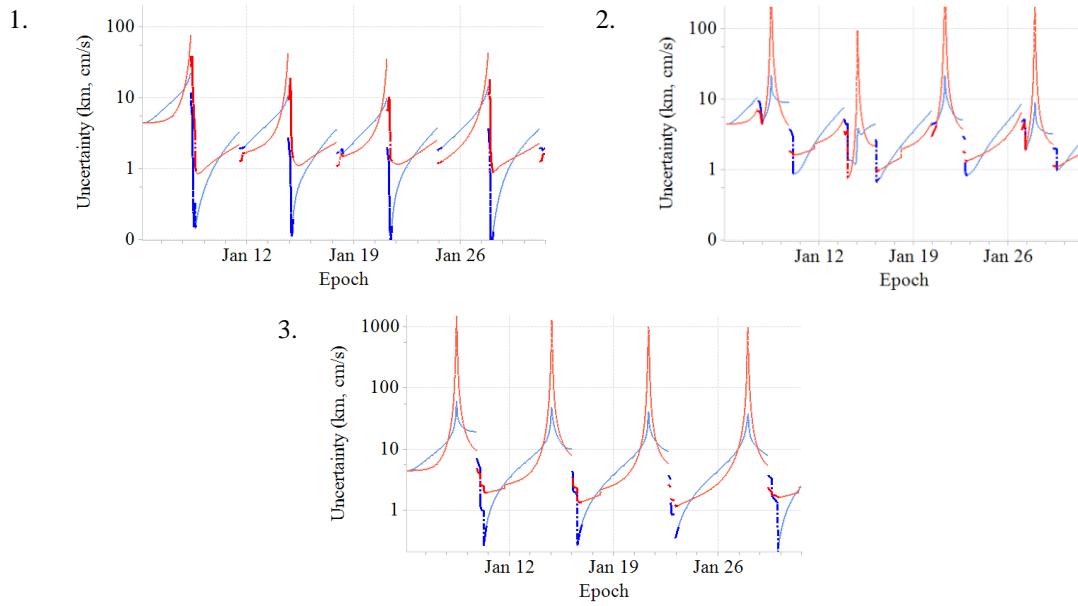


Figure 8. Position (blue) and velocity (red) uncertainties for the corresponding tracking schedules. Times of active DSN tracking are in bold.

A Monte Carlo analysis is run to assess the uncertainties over many trials. Mean and maximum values of state error at perilune, state error at the stationkeeping (SK) epoch, maneuver estimation error, and total DV over nine revolutions appear in Table 9. Considering position error at perilune, tracking schedule 1 intuitively has the best state resolution at perilune, as a DSN pass is centered over perilune passage. Tracking schedule 3 yields the worst state resolution at perilune. Conversely, tracking schedule 3 results in the best state position resolution at the stationkeeping targeting epoch. As noted above, while the three tracking schedules yield significantly different uncertainties near perilune, sensitivity to tracking schedule selection is small in maneuver estimation error and total DV.

Table 7. Perilune error, stationkeeping targeting epoch state error, maneuver estimation error and stationkeeping maneuver statistics for different DSN tracking schedules.

Tracking Schedule	Perilune Position Error mean/max (m)	Perilune Velocity Error mean/max (cm/s)	SK Solve Position Error mean/max (m)	SK Solve Velocity Error mean/max (cm/s)	Maneuver Estimation Error mean / max (cm/s)	Total DV mean/max (cm/s)
1	180 / 1816	6.9 / 73.9	1878 / 27165	1.0 / 24.0	13.5 / 35.5	88.9 / 106.0
2	4541 / 48275	118.8 / 1304.2	232.2 / 1458.2	0.3 / 1.8	14.0 / 39.8	92.7 / 102.6
3	23566 / 291350	622.0 / 7756.0	158.9 / 1263.4	0.5 / 3.9	13.7 / 38.0	92.5 / 99.2

OD SUPPLEMENTAL CRATER VISUAL MEASUREMENTS

The Gateway’s southern L2 NRHO places its perilune over the lunar north pole, where it sweeps over the lunar northern hemisphere in under six hours. While holding SPEA with the solar panels aligned in the inertial Z direction, the Gateway has close and quickly moving views of lunar north pole craters from its body frame $-Z$ faces.

Optical navigation observations employ cameras with feature recognition and measuring software to convert 2D images into measurements that can be processed in a navigation filter for spacecraft orbit determination. A camera fixed to the $-Z$ face of the Gateway could process views of craters with known locations and dimensions into one-way range and angle measurements.

As seen in Figure 10 and Table 9, velocity uncertainty increases sharply in the vicinity of perilune, and the trajectory of the Gateway in its NRHO is most sensitive to perturbations near perilune, thus additional tracking measurements in this neighborhood are valuable to decrease uncertainty near perilune. To test this hypothesis, representative groundstations are simulated in the centers of two northern hemisphere craters and measurements are taken between the craters and the Gateway, and processed along with DSN range and range rate measurements.

In a similar manner to the previous study, DSN passes are placed on the NRHO in differing geometries and supplemented with optical observations to the northern craters. The DSN passes are supplemented with range and angle measurements to two near-north pole craters. The choice of craters is likely to be a significant design element, but for the broad purpose of this study two craters with significant distance between them are chosen to maximize the geometric advantage of measurements. Specifically, craters Hermite and Schwarzschild are utilized for the current study.

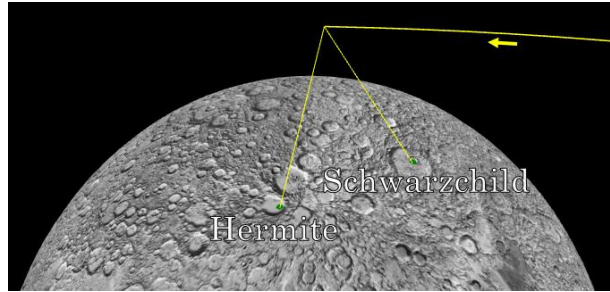


Figure 9. A depiction of the Gateway trajectory passing over and observing the Hermite and Schwarzschild craters.

The Gateway’s trajectory is propagated, DSN and crater observations are simulated, and an estimated Gateway’s state is processed in a SRIF using the simulated measurements. The

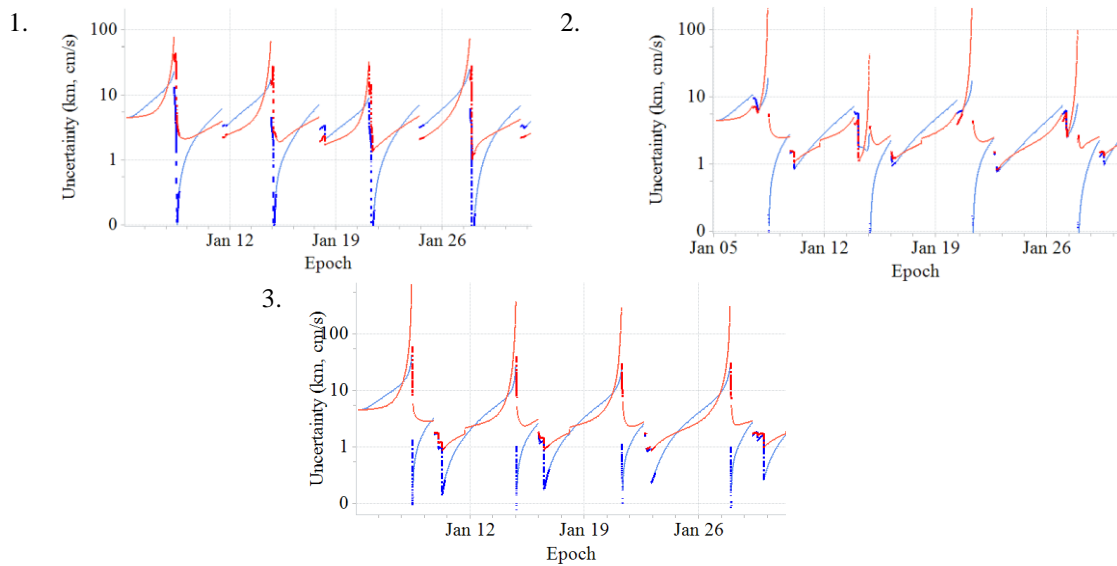


Figure 10. Position (blue) and velocity (red) uncertainties for the corresponding tracking schedules, with additional crater passes over perilune. Times of active tracking are in bold.

Table 10 summarizes a comparison of the OD performance, maneuver estimation error, and maneuver costs for the DSN schedules augmented with optical observations of craters while over perilune. The inclusion of optical measurements in the vicinity of perilune naturally improves the state resolution at that

epoch. There are modest improvements in state error at the stationkeeping targeting epoch, but this doesn't translate into improved maneuver estimation or total DV.

Table 8. Perilune error, stationkeeping targeting epoch state error, maneuver estimation error and stationkeeping maneuver statistics for different DSN tracking schedules augmented with optical measurements to north pole craters.

Tracking Schedule	Perilune Position Error mean/max (m)	Perilune Velocity Error mean/max (cm/s)	SK Solve Position Error mean/max (m)	SK Solve Velocity Error mean/max (cm/s)	Maneuver Estimation Error mean / max (cm/s)	Total DV mean/max (cm/s)
1	35 / 301	3.6 / 37.3	1723 / 14819	1.2 / 12.6	14.3 / 34.1	93.7 / 105.3
2	22 / 115	1.6 / 13.1	196.4 / 945.4	0.2 / 0.76	13.9 / 36.1	92.7 / 102.2
3	52 / 1205	6.6 / 166.5	84.2 / 695.7	0.2 / 2.81	13.9 / 39.7	93.7 / 113.7

Reducing and Eliminating DSN Coverage

While there doesn't seem to be much sensitivity to the addition of crater measurements on the resultant stationkeeping targeting accuracy or efficiency, the results suggest that the orbit could be maintained with fewer observations altogether, or possibly entirely autonomously. To investigate this possibility, three similar tracking plans are compared. Below in Figure 11 are the position and velocity uncertainty traces over time. Figure 11.1 shows both a crater pass and a pre-stationkeeping targeting 8 hour DSN pass, figure 11.2 shows only the DSN pass, and figure 11.3 shows the case with crater observations only.

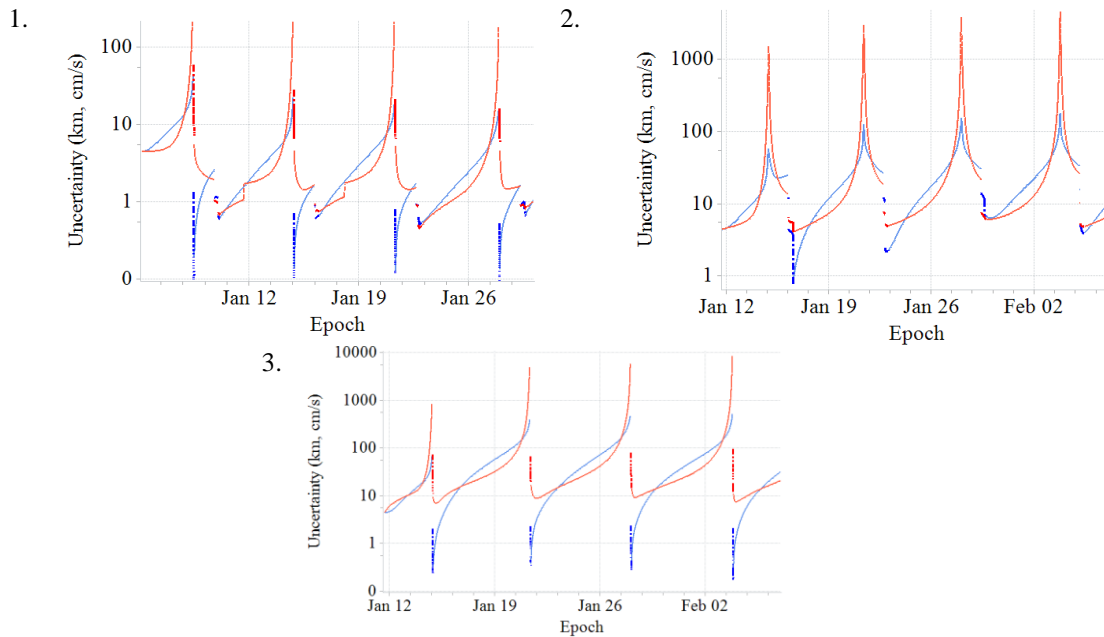


Figure 11. Position (blue) and velocity (red) uncertainties for the corresponding tracking schedules, with reduced or excluded DSN tracking. Times of active tracking are in bold.

After some tuning with the velocity process noise, it was possible to maintain the NRHO using only observations to the Hermite and Schwarzschild craters. Below in Table 9 are the perilune uncertainty statistics and stationkeeping targeting performance statistics.

Table 9. . Perilune error, stationkeeping targeting epoch state error, maneuver estimation error and stationkeeping maneuver statistics for different tracking schedules with reduced or no DSN coverage.

<i>Tracking Schedule</i>	<i>Perilune Position Error mean/max (m)</i>	<i>Perilune Velocity Error mean/max (cm/s)</i>	<i>SK Solve Position Error mean/max (m)</i>	<i>SK Solve Velocity Error mean/max (cm/s)</i>	<i>Maneuver Estimation Error mean / max (cm/s)</i>	<i>Total DV mean/max (cm/s)</i>
1						
2						
3						

While it's possible to maintain the NRHO using optical observations to northern pole craters only, the performance is worse, and there are cases that would require intervention to maintain SRIF lock on the state estimate. A deeper look into the expected performance of a camera system, and ability to utilize different crater geometries could improve the performance of optical autonomous navigation in NRHO.

CONCLUSIONS

This paper describes a possible construction path of the Gateway and simulates each configuration of the Gateway during assembly to gather attitude performance and propellant use statistics for the mission. Human lunar lander missions with a three-piece lunar lander concept going through the Gateway are simulated, and their propellant use statistics described. A range of possible total hydrazine propellant budgets are presented with varying assumptions on the mix of Gateway or lunar surface missions post-completion. The total propellant budget presented drives initial hydrazine load requirements and may also drive the necessity of hydrazine refueling during or after construction.

The OD performance gains achieved by processing additional optical data near perilune returns mixed results. There is not a strong indication that the addition of optical observations around perilune can drive accuracy days later when the stationkeeping maneuver is solved. The optical measurements do reduce Gateway state uncertainty and error in the vicinity of perilune, which has value to disposals from there. A diagnosis of the results is underway, and some solutions are detailed in the next section.

FORWARD WORK

As the Gateway matures and selections are made for element designs, the analysis will need to be continually refined in cycles. This paper assumes a three-piece lander concept, which may change as selections are made. Cislunar transfers of the Gateway are envisioned as a part of its mission, which would include prolonged SEP thrust arcs that drive attitude and in turn hydrazine budget. A future analysis can look into the cost of holding non-SPEA attitudes for thrusting arcs, and strategies to reduce hydrazine use while successfully executing the desired transfer. There is a significant chance of a refueling mission which could require a time in which the Gateway cannot change attitude or perform a maneuver while the fuel transfer takes place. The recovery from this condition would need to be analyzed and budgeted. On-orbit mission slews away from SPEA for various reasons need investigation for feasibility and cost. These slews include a "barrel roll" over the perilune for thermal contingency reasons, as well as for window viewing reasons. A side quest will be investigating the feasibility of incorporating Orion's RCS thrusters into Gateway attitude control.

Stationkeeping targeting performance is insensitive to the tracking schedules explored or the inclusion of optical measurements near perilune. It is possible that differences in propagation models for the estimated and truth spacecraft are causing errors that reduce the accuracy of stationkeeping targeting. Directed and timed perturbations like vents can be modeled into the estimated trajectory to reduce error. Different tracking schedules, and constant tracking with crewed Gateway will be evaluated, as well as different crater lo-

cations and tracking geometries. Finally, the measurement model for optical observations needs to be refined to more closely match how these systems will perform on mission.

ACKNOWLEDGMENTS

The authors would like to thank Gary Brown for his input. Portions of this work were completed at NASA JSC through contract #NNJ13HA01C.

REFERENCES

- ¹ Whitley, R. and R. Martinez, "Options for Staging Orbits in Cislunar Space," IEEE Aerospace 2015, Big Sky Montana, March 2015.
- ² Whitley, R.J., D.C. Davis, M.L. McGuire, L.M. Burke, B.P. McCarthy, R.J. Power, K.C. Howell, "Earth-Moon Near Rectilinear Halo and Butterfly Orbits for Lunar Surface Exploration", AAS/AIAA Astrodynamics Specialists Conference, Snowbird, Utah, August 2018.
- ³ Zimovan, E., K. C. Howell, and D. C. Davis, "Near Rectilinear Halo Orbits and Their Application in Cis-Lunar Space," 3rd IAA Conference on Dynamics and Control of Space Systems, Moscow, Russia, May-June 2017.
- ⁴ Davis, D. C., S. A. Bhatt, K. C. Howell, J. Jang, R. L. Whitley, F. D. Clark, D. Guzzetti, E. M. Zimovan, and G. H. Barton, "Orbit Maintenance and Navigation of Human Spacecraft at Cislunar Near Rectilinear Halo Orbits," 27th AAS/AIAA Space Flight Mechanics Meeting, San Antonio, Texas, February 2017.
- ⁵ Guzzetti, D., E. M. Zimovan, K. C. Howell, and D. C. Davis, "Stationkeeping Methodologies for Spacecraft in Lunar Near Rectilinear Halo Orbits," AAS/AIAA Spaceflight Mechanics Meeting, San Antonio, Texas, February 2017.
- ⁶ Davis, D. C., S. M. Phillips, K. C. Howell, S. Vutukuri, and B. P. McCarthy, "Stationkeeping and Transfer Trajectory Design for Spacecraft in Cislunar Space," AAS/AIAA Astrodynamics Specialists Conference, Stevenson, Washington, August 2017.
- ⁷ Newman, C. P., D. C. Davis, R. J. Whitley, J. R. Guinn, and M. S. Ryne, "Stationkeeping, Orbit Determination, and Attitude Control for Spacecraft in Near Rectilinear Halo Orbit," AAS/AIAA Astrodynamics Specialists Conference, Snowbird, Utah, August 2018.
- ⁸ D'Souza, C. and G. Barton, "Process Noise Assumptions for Orion Cislunar Missions," NASA Technical Brief, August 2016.
- ⁹ Markley, F.L., R.G. Reynolds, F.X. Liu, and K.L. Lebsack, "Maximum torques and momentum envelopes for reaction-wheel arrays," Journal of Guidance, Control, and Dynamics, Vol. 33, No. 5, 2010.